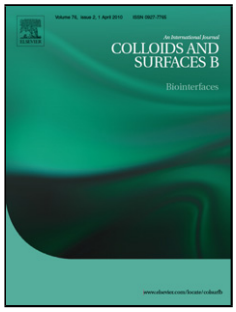

Title: CuO nanoparticles incorporated in hierarchical MFI zeolite as highly active electrocatalyst for non-enzymatic glucose sensing

Author: Junping Dong Taolei Tian Linxiao Ren Yuan Zhang Jiaqiang Xu Xiaowei Cheng

PII: S0927-7765(14)00650-X
DOI: http://dx.doi.org/doi:10.1016/j.colsurfb.2014.11.027
Reference: COLSUB 6750

To appear in: *Colloids and Surfaces B: Biointerfaces*

Received date: 13-8-2014
Revised date: 24-10-2014
Accepted date: 18-11-2014

Please cite this article as: J. Dong, T. Tian, L. Ren, Y. Zhang, J. Xu, X. Cheng, CuO nanoparticles incorporated in hierarchical MFI zeolite as highly active electrocatalyst for non-enzymatic glucose sensing, *Colloids and Surfaces B: Biointerfaces* (2014), http://dx.doi.org/10.1016/j.colsurfb.2014.11.027

CuO nanoparticles incorporated in hierarchical MFI zeolite as highly active electrocatalyst for non-enzymatic glucose sensing

Junping Dong[*a,b], Taolei Tian[a], Linxiao Ren[a], Yuan Zhang[a,b], Jiaqiang Xu[a], Xiaowei Cheng[*c]

[a] Department of Chemistry, College of Science, Shanghai University, Shanghai 200444, China

[b]State Key Laboratory of Transducer Technology, Shanghai Institute of Microsystem and Information Technology, Chinese Academy of Sciences, Shanghai 200050, China

[c] Department of Chemistry and Shanghai Key Laboratory of Molecular Catalysis and Innovative Materials, Fudan University, Shanghai 200433, China

* Corresponding Authors:

E-mail: jpdong@shu.edu.cn ; xwcheng@fudan.edu.cn

Tel.: +86 21 66132930

ABSTRACT

A hierarchical MFI zeolite，with typical micro/meso bimodal pore structures, was prepared by desilication method. CuO nanoparticles (NPs) were incorporated into the hierarchical MFI zeolite by impregnation method. CuO/hierarchical zeolite composites were characterized by X-ray diffraction, transmission electron microscopy and nitrogen sorption. It is shown that the CuO nanoparticles are mostly dispersed in the mesopores with remaining of the crystallinity and morphology of the host zeolite. CuO nanoparticles located in hierarchical zeolite exhibit the excellent electrocatalytic performances to oxidation of glucose in alkaline media. The electrocatalytic activity enhances with increasing the loading content of CuO from 5% to 15%. The composites were fabricated for nonenzyme glucose sensing. Under the optimal conditions, the sensor shows a wide linear range from 5×10^{-7} to 1.84×10^{-2} M with a low detection limit of 3.7×10^{-7} M. The sensor also exhibits good repeatability, long-term stability as well as high selectivity against interfering species.

Keywords: CuO; Hierarchical zeolite; Glucose; Non-enzymatic biosensor; electrocatalyst

1. Introduction

Nowadays, the fast determination of glucose is considered to be important in wide areas of food industry, biotechnology and clinical diagnostics. Especially for the patients with diabetes mellitus, the regular test of glucose level is also necessary, which demands glucose sensors with high sensitivity, good reliability and excellent selectivity. Glucose oxidase (GOD)-based electrochemical biosensors have been proved to be a powerful device for glucose determination thanks to the high selectivity, sensitivity and low detection limit. However, due to the intrinsic feature of enzymes, there are some drawbacks in the GOD-based biosensors, such as poor reproducibility, thermal and chemical instability [1, 2]. Therefore, the non-enzymatic glucose biosensors based on metal nanoparticles (Au, Pt, Pd, Cu, Ni), metal oxides (Co_3O_4, CuO, NiO) or alloys (Pt/Pb, Pt/Au, Au/Ag) [3-10] have received more and more attentions. Non-enzymatic glucose biosensors alleviated the problems of enzyme-based biosensors such as insufficient stability, lower reproducibility, thermal and chemical instability, sensitivity to temperature, pH and humidity. Hence it will probably become the fourth generation glucose sensors for the future analytical applications.

Non-enzymatic glucose biosensors are based on the glucose oxidation catalyzed by a variety of electrocatalysts. Therefore, the preparation of electrocatalysts with high performance is crucial for improving sensitivity, selectivity and reliability of sensors. Copper oxide (CuO) nanoparticles, as a well-known p-type semiconductor, has gained increasing attention due to its low production cost, high stability, good electrical conductivity and easy availability, and more importantly, CuO nanoparticles possess the excellent electrocatalytic activity to reduction of H_2O_2 and oxidation of glucose as well as purine and amino acid [9, 11-15]. Except that, a series of CuO nanocomposites

based on various substrates have been developed for non-enzymatic glucose sensors [16-18]. In recent years, some novel host materials, such as graphene, carbon nanotubes, ordered mesoporous silica-based materials, etc., are widely applied as hosts for electrocatalysis and further construction of biosensors owing to their large surface area and good biocompatibility [19-22].

In this work, hierarchical zeolite, another novel type of silica-based matrix, was prepared by desilication of microporous MFI zeolite in alkaline media [23]. As we know, microporous MFI zeolite has definite shape and unique crystal structures, but usually it cannot be applied for construction of biosensors duo to the smaller pores (<1 nm). The desilication method by base leaching has already been proved to be able to create extra mesopores (10-30 nm) in addition to the intrinsic micropores [24]. The hierarchical zeolite is highly desired in catalysis fields [25] and is becoming attractive in biosensing application. This type of hierarchical zeolite with micro/meso pore structures not only possesses mesopores induced by desilication, but also offers the interconnected three-dimensional pore systems. The larger mesopores are favorable for biomolecules immobilization or high loading of nanoparticles, and the interconnected three-dimensional pore structures can provide a convenient and fast pathway for mass transfer. Recently, Ren and co-authors [26] dispersed gold nanoparticles (AuNPs, 3-20 nm) into the hierarchical zeolite, which was used as a novel matrix for the immobilization of hemoglobin protein to construct H_2O_2 biosensor.

Herein, we incorporated high content of CuO nanoparticles (~15%) in hierarchical MFI zeolite by the simple wet impregnation method. The CuO/hierarchical zeolite composites were applied as highly reactive electrocatalyst for glucose oxidation and further constructed a non-enzymatic glucose biosensor. The sensor exhibits the excellent performance such as high sensitivity, low

detection limit and good selectivity.

2. Experimental

2.1. Synthesis of CuO incorporated hierarchical porous MFI zeolite composites

The parent MFI zeolite used in this work is commercially available with a nominal Si/Al ratio of 50. The hierarchical MFI zeolite with micro/meso pore structures (denoted as meso-MFI), were prepared by treatment of microporous MFI zeolite in NaOH solution as described in detail elsewhere [23]. The incorporation of CuO NPs was performed by impregnation of 1.0 g meso-MFI zeolite into 10 g of $Cu(NO_3)_2$ aqueous solution with different concentrations at 90 ^oC over 3 h under stirring. The mixtures were then slowly dried at 60 ^oC for 6 h. Subsequently the solid sample were annealed in air at 550 ^oC for 5 h, which was labeled as meso-MFI-xCuO, in which x represents the mass ratio of CuO to zeolite powder.

2.2. Fabrication of modified carbon paste electrode

The modified carbon paste electrode was prepared as follows: 50 mg meso-MFI-xCuO composites, 0.5 g carbon graphite and 0.4 g liquid paraffin were uniformly mixed and carefully grounded in an agate mortar. The resulting homogeneous pastes were then packed into a cavity (3 mm diameter) at the end of a glass tube. Electrical contact was made by a fine copper wire contacted to one side of the carbon paste. The resulting carbon paste electrode was finally polished and smoothed on a weighting paper.

2.3. Apparatus and measurements

Powder X-ray diffraction measurements were performed with a Rigaku D-MAX/IIA X-ray diffractometer in a scanning range of 5–70° (2θ) at a rate of 4° (2θ)/min with Cu Kαradiation. Transmission electron microscope (TEM) images were obtained on a JEOL 2011 instrument. Nitrogen sorption isotherms were carried out on a Micromeritics ASAP2020M+C instrument. All electrichemical experiments were preformed on CHI 660C electrochemical workstation (Chenhua, Shanghai, China) with a conventional three-electrode system, where the modified carbon paste electrodes as working electrode, a platinum wire as auxiliary electrode and a Ag/AgCl (3M KCl) electrode as reference electrode. All solutions in the cell were deoxygenated by highly purified nitrogen gas for at least 15 min prior to experiments and a nitrogen atmosphere was then kept over the solution during measurements.

3. Results and discussion

3.1. Characterization of meso-MFI-xCuO composites

Fig. 1 here

The X-ray diffraction patterns of meso-MFI zeolite after loading different content of CuO were shown in Fig. 1A. Compared with meso-MFI zeolite (curve a in Fig. 1A), all meso-MFI-xCuO composites can keep the typical MFI crystal structure after CuO NPs are incorporated into the hierarchical zeolite, except for the slight decreasing of peak intensity. In contrast with the standard diffraction patterns for CuO (JCPDS 045-0937), the diffraction peaks at 35.5°, 38.7°and 48.7°/2θ (denoted as the symbol of ▽) for meso-MFI-xCuO composites are assigned to that of monoclinic CuO crystals. Furthermore, the diffraction intensity of CuO increases as the loading of CuO NPs in meso-MFI zeolite from 5% to 15% (curves b-d in Fig. 1A).

N_2 physical sorption analysis is used to evaluate pore structures of meso-MFI zeolite before and after the incorporation of CuO. Fig. 1B displayed N_2 sorption isotherms of two samples and the textural properties of samples were shown in Table 1.

The parent meso-MFI shows a type IV isotherm with a sharp N_2 uptake at a lower relative pressure of P/P_0 = 0.45, which suggests the presence of open mesopores connected to the outer surface (curve a in Fig. 1B). The inset is pore size distribution of the parent meso-MFI. The main pore size is about 20 nm for meso-MFI zeolite. This result indicates that desilication process generates the expected mesopores on the surface of microporous MFI zeolite. After 15% CuO loading on meso-MFI, it is noted that both surface areas and pore volumes of the sample significantly decrease (shown in Table 1). The BET surface areas change from 267 to 135 m^2/g and pore volumes from 0.286 to 0.087 cm^3/g, respectively. The significant decreases in surface areas and pore volumes, especially in mesoporous volumes, imply that most of the CuO NPs are introduced successfully into the mesopores on MFI zeolite.

Fig. 2 here

Fig. 2 showed the TEM images of meso-MFI-xCuO. All meso-MFI zeolite samples display the typical coffin shape similar to that of microporous MFI zeolite. Some bright spots can be clearly observed within the single crystal, indicating the presence of mesopores caused by desilication. Seen from high magnification images in Fig. 2B and 2D, when 5% or 10% of CuO NPs are embedded into meso-MFI, the fine CuO NPs (dark spots) are well located inside the cavities of meso-MFI with a size distribution of 10-30 nm. When the loading of CuO is increased up to 15% (Fig. 2F), more CuO NPs are confined inside the cavities of meso-MFI zeolite, and some of them aggregate and grow larger. This result is well consistent with the XRD pattern of meso-MFI-15% CuO (Fig. 1c), in which the strong diffraction peaks of CuO are clearly visible due to a larger

number of CuO NPs in meso-MFI.

3.2. Electro-oxidation activity of glucose on different porous silica materials

Fig. 3 here

Electrocatalytic oxidation of glucose was compared on three different porous silica materials. SBA-15, a kind of representative mesoporous silica material, could provide one-dimensional pore channels and well-ordered mesopores with pore size of 7 nm. The pristine MFI zeolites (or ZSM-5 zeolite) are microporous crystalline aluminosilicates composed of two-dimensional channels with straight channels (5.3*5.6 Å) parallel to b-axis, interconnected to sinusoidal channels (5.0*5.5 Å). From Fig. 3 it is found that meso-MFI zeolite exhibits the highest response current for oxidation of glucose when the equal amount of CuO is incorporated in pores, indicating that meso-MFI with bimodal pore structures combined with the larger mesopores are advantageous over that one-dimensional SBA-15 and microporous MFI zeolite.

3.3. Electrocatalytic oxidation of glucose on meso-MFI-15%CuO modified electrode

The oxidation of glucose was performed on meso-MFI-15%CuO modified electrode using cyclic voltammetry (CV) and linear sweep voltammetry (LSV).

Fig. 4 here

Fig. 4A showed the cyclic voltammograms of the meso-MFI-15% CuO modified electrode in the presence and absence of glucose. Some redox transitions appear and are indicated by peaks I to VI in the potential region from -0.9 to 0.9 V. The anodic peaks I and II represent the oxidation

from Cu (0) to Cu (I) and Cu (I) to Cu (II) respectively, while the corresponding cathodic peaks V and VI in the reverse scan are due to the transition of Cu (II) to Cu (I) and Cu (I) to Cu (0), which are the typical characteristics of CuO materials [21, 27]. Peak III is considered to be related with the formation of soluble species $HCuO_2^-$.

When the 5 mM glucose is added in the NaOH electrolyte, a visible shoulder wave centered at 0.6 V is responsible for the electrooxidation of glucose where Cu (III) and hydroxyl radicals are probably involved [27, 28]. Moreover, in the cathodic scan, the disappearance of peak IV provides evidence that the Cu (III) is consumed in the electrooxidation of glucose.

The electrocatalytic oxidation process of glucose in the alkaline electrolyte at the CuO electrodes is generally considered undergoing several steps [28-31]:

Firstly, CuO is electrochemically oxidized to strong oxidizing Cu (III) species such as CuOOH or $Cu(OH)_4^-$:

$CuO + OH^- \rightarrow CuOOH + e^-$ or $CuO + H_2O + 2OH^- \rightarrow Cu(OH)_4^- + e^-$

And then, glucose is catalytically oxidized by the Cu (III) species and produces gluconic acid.

Cu (III) + glucose + $e^- \rightarrow$ Cu (II) + gluconolactone; gluconolactone→gluconic acid (hydrolysis)

Fig. 4B recorded the linear sweep voltammograms of meso-MFI-15%CuO electrode to the different concentrations of glucose. When glucose is added, a distinct anodic peak appears at around 0.6 V. Successive increments of the glucose result in the gradual increase of response current.

The effect of scan rates on the anodic currents of glucose was tested by linear sweep voltammetry at the meso-MFI-15%CuO modified electrode (Fig. 4C). In the range of 5–50 mV s^{-1}, the peak currents (I_{pa}) vary linearly with the scan rates (v) with a correlation coefficient of 0.991.

The linear regression equation is expressed as I_{pa} (μA) = 16.57 + 0.19 ν (mV s^{-1}). This result verifies that the oxidation reaction is controlled by the surface adsorption of glucose molecules.

3.4. Amperometric detection of glucose

Fig. 5 here

The accurate detection of glucose was carried out at meso-MFI-15%CuO electrode. Fig. 5A displayed the current–time curve with successive injections of glucose in 100 mM NaOH electrolyte at 0.65 V. The upper left insets showed the original segment of amperometric curve after addition of the lower concentration of glucose. As expected, with each addition of glucose to stirred NaOH solution, the oxidation currents rise steeply and the current value achieves 95% of the steady-state current within 5 s. The calibration curve for glucose sensor was shown in Fig. 5B. The response currents of the sensor are linearly dependent on the concentration of glucose in the range of 0.5 μM—18.4 mM with a fitting equation: I (μA) = 3.00 + 6.03$C_{glucose}$ (mM) (R^2=0.9997). Thus, the sensitivity of prepared sensor is 85.35 μA mM^{-1} cm^{-2}, and the detection limit is estimated to be 0.37 μM (S/N=3).

Meso-MFI-15% CuO electrode was compared with non-enzymatic glucose sensors based on Cu or Cu oxide nanomaterials in Table 2. It is obvious that the meso-MFI-15%CuO sensor exhibits good performances in terms of wide linear range and low detection limit.

3.5. Optimization for glucose sensor

The various factors influencing the responses of the sensor were investigated. It is known that

the alkalinity plays the important roles on electrocatalytic oxidation of glucose at CuO based nanomaterials. So the concentration of NaOH for glucose sensing was first optimized.

Fig. 6 here

Fig. 6A showed the amperometric responses of meso-MFI-15%CuO modified electrode to 0.5 mM glucose in various concentration of NaOH solution at applied potential of 0.65V. When the concentrations of NaOH solution increase from 20 mM to 200 mM, the response currents increase accordingly and then decreases in 200 mM. A maximum response current can be obtained in 100 mM NaOH.

Furthermore, the effect of the applied potentials on the response currents of the sensor was illustrated in Fig. 6B. In the range of 0.55V—0.7V, the oxidation currents of glucose increase with increasing applied potentials. However, further increasing potential, the side reaction takes place on the electrode surface, leading to the increase of the background current and then inhibition of glucose oxidation. Additional, some interfering species (such as ascorbic acid, uric acid, and dopamine) would be oxidized under higher potential to generate some intermediates, probably hindering glucose oxidation. From Fig. 6B, potential of 0.65 V is optimal for glucose sensing.

The current responses of meso-MFI-xCuO modified electrodes with different CuO loadings to 0.5 mM glucose were examined in Fig. 6C. It is found that the parent meso-MFI exhibits weak catalytic activities to glucose. When the different amounts of CuO are introduced into hierarchical MFI zeolite, the response currents increase apparently. Moreover, the response current at 15% CuO electrode is 7 times higher than that at 0% CuO electrode. Hence the integration of parent meso-MFI and CuO nanoparticles increases the sensitivity of the constructed sensor.

3.6. Anti-interference, repeatability and stability of the meso-MFI-15% CuO sensor

The selectivity of a sensor is very important for practical application. Usually, some electroactive species commonly present in physiological samples such as ascorbic acid (AA), dopamine (DA) and uric acid (UA) may interfere with the accurate determination of glucose. Ordinaryly, the normal physiological level of glucose is about 3–8 mM and the interfering species such as AA, UA and DA are less than 0.1mM [41]. The interference experiment was carried out by adding 0.1 mM interfering species into 2.0 mM glucose in 100 mM NaOH as shown in Fig. S1 (Supplementary materials).

The addition of 0.1mM UA does not influence the detection of 2.0 mM glucose, whereas the presence of 0.1 mM AA and 0.1 mM DA induces the larger current responses in I-T curves. However, when a layer of 5% Nafion film was coated on the meso-MFI-15% CuO modified carbon paste electrode, the amperometric responses of AA and DA could decrease to 6.0% and 4.2%, respectively.

The repeatability and stability of glucose sensor were also evaluated. The relative standard deviation (RSD) is 4.12% for five newly fabricated biosensors. The current responses of ten successive measurements to 0.5 mM glucose yield an RSD of 2.36% at one chosen meso-MFI-15% CuO modified carbon paste electrode. When the modified electrode is not used, it is wrapped with a piece of thin plastic film and stored at 4^{o}C. After two weeks, the current response of meso-MFI-15% CuO modified electrode just losses 1.6% of its original current. The good reproducibility and long term stability of meso-MFI-15% CuO electrode are owing to the chemically stable CuO phase located in the hierarchically porous MFI zeolite.

Finally, the sensor was applied to the determination of glucose in real blood serum samples.

Here serum sample was firstly diluted by 5 times and then 25 uL diluted sample was added to 25 ml of 100 mM NaOH solution, and the current response was recorded at 0.65V. The data from the fabricated glucose sensor are 4.38 mM (average for three measurements), close to the result of 4.2 mM from a spectrophotometric method performed in a local hospital.

4. Conclusions

CuO nanoparticles entrapped in hierarchical MFI zeolite were successfully developed as a novel sensing material to construct a sensitive, low cost non-enzymatic glucose biosensor. The electrochemical study reveals that the sensor based on meso-MFI-xCuO displays excellent catalytic activity towards glucose oxidation as increasing loading of CuO. Under the optimized conditions, the newly constructed non-enzymatic glucose sensor presents the attractive features such as wide linear range, low detection limit, excellent stability and selectivity. These significantly improved performances are ascribed to the synergistic effect of two significant factors: (i) the unusual electrocatalytic activity of the entrapped CuO nanoparticles endows the sensor a satisfied performance and (ii) the inherent catalytic properties of meso-MFI zeolite towards glucose oxidation combined with its special hierarchical structure, in which larger mesopores could accommodate more catalytic active molecules, and interconnected three-dimensional pore systems provide a facile and fast diffusion pathway for reactants or electrolyte ions.

Acknowledgements

This work is financed by National Natural Science Foundation of China (No. 21001027 and

61071040).

References

[1] K. Krikstopaitis, J. Kulys, L. Tetianec, Bioelectrocatalytical glucose oxidation with phenoxazine modified glucose oxidase, Electrochem. Commun. 6 (2004) 331.

[2] T. W. Tsai, G. Heckert, L. F. Neves, Y. Tan, D.Y. Kao, R. G. Harrison, D. E. Resasco, David W. Schmidtke, Adsorption of glucose oxidase onto single-walled carbon nanotubes and its application in layer-by-layer biosensors, Anal. Chem. 81 (2009) 7917–7925.

[3] P. Si, Y. Huang, T. Wang, J. Ma, Nanomaterials for electrochemical non-enzymatic glucose biosensors, RSC Adv. 3 (2013) 3487-3502.

[4] G. Wang, X. He, L. Wang, A. Gu, Y. Huang, B. Fang, B. Geng, X. Zhang, Non-enzymatic electrochemical sensing of glucose, Microchim. Acta 180 (2012) 161-186.

[5] X. Bo, J.C. Ndamanisha, J. Bai, L. Guo, Nonenzymatic amperometric sensor of hydrogen peroxide and glucose based on Pt nanoparticles/ordered mesoporous carbon nanocomposite, Talanta 82 (2010) 85-91.

[6] L.M. Lu, L. Zhang, F.L. Qu, H.X. Lu, X.B. Zhang, Z.S. Wu, S.Y. Huan, Q.A. Wang, G.L. Shen, R.Q. Yu, A nano-Ni based ultrasensitive nonenzymatic electrochemical sensor for glucose: enhancing sensitivity through a nanowire array strategy, Biosens. Bioelectron. 25 (2009) 218-223.

[7] Y.X. Liu, Y. Ding, Y.C. Zhang, Y. Lei, Pt–Au nanocorals, Pt nanofibers and Au microparticles prepared by electrospinning and calcination for nonenzymatic glucose sensing in neutral and alkaline environment, Sens. Actuators B 171 (2012) 954-961.

[8] M. Tominaga, T. Shimazoe, M. Nagashima, H. Kusuda, A. Kubo, Y. Kuwahara, I. Taniguchi, Electrocatalytic oxidation of glucose at gold-silver alloy, silverand gold nanoparticles in an alkaline solution, J. Electroanal. Chem. 590 (2006) 37-46.

[9] Y. Zhang, Y. Liu, L. Su, Z. Zhang, D. Huo, C. Hou, Y. Lei, CuO nanowires based sensitive and selective non-enzymatic glucose detection, Sens. Actuators, B 191 (2014) 86-93.

[10] P. Si, X. Dong, P. Chen, D. Kim, A hierarchically structured composite of Mn_3O_4/3D graphene foam for flexible nonenzymatic biosensors, J. Mater. Chem. B, 1 (2013) 110-115.

[11] L. Zhang, H. Li, Y. Ni, J. Li, K. Liao, G. Zhao, Porous cuprous oxide microcubes for

non-enzymatic amperometric hydrogen peroxide and glucose sensing, Electrochem. Commun. 11 (2009) 812-815.

[12] X. Zhang, X. Liang, M. Xu, X. Bao, F. Wang, Z. Yang, Electrodeposit nano-copper oxide on glassy carbon electrode for simultaneous detection of guanine and adenine, J. Appl. Electrochem. 42 (2012) 375-381.

[13] G. Casell, T. R. I. Cataldi, A. Guerrier, E. Desimoni, Copper dispersed into polyaniline films as an amperometric sensor in alkaline solutions of amino acids and polyhydric compounds, Anal. Chim. Acta 335 (1996) 217-225.

[14] P. S. S. Berchmans, Copper oxide modified glassy carbon electrode prepared through copper hexacyanoferrate–G5-PAMAM dendrimer templates as electrocatalyst for carbohydrate and alcohol oxidation, J. Solid State Electrochem. 16 (2011) 1527-1535.

[15] D. J. Chen, Y. H. Lu, A. J. Wang, J. J. Feng, T. T. Huo, W. J. Dong, Facile synthesis of ultra-long Cu microdendrites for the electrochemical detection of glucose, J. Solid State Electrochem. 16 (2011) 1313-1321.

[16] X. Y. Yang, G. Tian, N. Jiang, B. L. Su, Immobilization technology: a sustainable solution for biofuel cell design, Energy Environ. Sci. 5 (2012) 5540.

[17] K. Tian, M. Prestgard, A. Tiwari, A review of recent advances in nonenzymatic glucose sensors, Mater. Sci. Eng. C 41 (2014) 100-118.

[18] C. L. Sun, W. L. Cheng, T. K. Hsu, C. W. Chang, J. L. Chang, J. M. Zen, Ultrasensitive and highly stable nonenzymatic glucose sensor by a CuO/graphene-modified screen-printed carbon electrode integrated with flow-injection analysis, Electrochem. Commun. 30 (2013) 91-94.

[19] N. Q. Dung, D. Patil, H. Jung, D. Kim, A high-performance nonenzymatic glucose sensor made of CuO-SWCNT nanocomposites, Biosens. Bioelectron. 42 (2013) 280-286.

[20] Y. W. Hsu, T. K. Hsu, C.-L. Sun, Y.T. Nien, N. W. Pu, M. D. Ger, Synthesis of CuO/graphene nanocomposites for nonenzymatic electrochemical glucose biosensor applications, Electrochim. Acta 82 (2012) 152-157.

[21] M. U. A. Prathap, B. Kaur, R. Srivastava, Direct synthesis of metal oxide incorporated mesoporous SBA-15 and their applications in non-enzymatic sensing of glucose, J. Colloid Interface Sci. 381 (2012) 143-151.

[22] Y. Deng, C. Deng, D. Qi, C. Liu, J. Liu, X. Zhang, D. Zhao, Synthesis of Core/Shell Colloidal Magnetic Zeolite Microspheres for the Immobilization of Trypsin, Adv. Mater. 21 (2009) 1377-1382.

[23] X.W. Cheng, Q.Y. Meng, J. Y. Chen, Y.C. Long, A facile route to synthesize mesoporous ZSM-5 zeolite incorporating high ZnO loading in mesopores, Microporous Mesoporous Mater. 153 (2012) 198-203.

[24] J. C. Groen, J. C. Jansen, J. A. Moulijn, J. Pérez-Ramírez, Optimal aluminum-assisted mesoporosity development in MFI zeolites by desilication, J. Phys. Chem. B 108 (2004) 13062-13065.

[25] M. S. Holm, E. Taarning, K. Egeblad, C.H. Christensen, Catalysis with hierarchical zeolites, Catal. Today 168 (2011) 3–16.

[26] L. Ren, J. Dong, X. Cheng, J. Xu, P. Hu, Hydrogen peroxide biosensor based on direct electrochemistry of hemoglobin immobilized on gold nanoparticles in a hierarchically porous zeolite, Microchim. Acta 180 (2013) 1333-1340.

[27] Y. Zhang, L. Su, D. Manuzzi, H.V. de los Monteros, W. Jia, D. Huo, C. Hou, Y. Lei, Ultrasensitive and selective non-enzymatic glucose detection using copper nanowires, Biosens. Bioelectron. 31 (2012) 426-432.

[28] J. Wang, W. D. Zhang, Fabrication of CuO nanoplatelets for highly sensitive enzyme-free determination of glucose, Electrochim. Acta 56 (2011) 7510-7516.

[29] L. Luo, L. Zhu, Z. Wang, Nonenzymatic amperometric determination of glucose by CuO nanocubes-graphene nanocomposite modified electrode, Bioelectrochemistry 88 (2012) 156-163.

[30] M. Tominaga, T. Shimazoe, M. Nagashima, H. Kusuda, A. Kubo, Y. Kuwahara, I. Taniguchi, Electrocatalytic oxidation of glucose at gold–silver alloy, silver and gold nanoparticles in an alkaline solution, J. Solid State Electrochem. 590 (2006) 37-46.

[31] V. Dharuman, K. Chandrasekara Pillai, RuO_2 electrode surface effects in electrocatalytic oxidation of glucose, J. Solid State Electrochem. 10 (2005) 967-979.

[32] S. Liu, J. Tian, L. Wang, X. Qin, Y. Zhang, Y. Luo, A. M. Asiri, A.O. Al-Youbi, X. Sun, A simple route for preparation of highly stable CuO nanoparticles for nonenzymatic glucose detection, Catal. Sci. Technol. 2 (2012) 813-817.

[33] J. Chen, L. Xu, R. Xing, J. Song, H. Song, D. Liu, J. Zhou, Electrospun three-dimensional porous CuO/TiO_2 hierarchical nanocomposites electrode for nonenzymatic glucose biosensing, Electrochem. Commun. 20 (2012) 75-78.

[34] A. Umar, M. M. Rahman, A. Al-Hajry, Y. B. Hahn, Enzymatic glucose biosensor based on flower-shaped copper oxide nanostructures composed of thin nanosheets, Electrochem. Commun. 11 (2009) 278-281.

[35] Y. J. Yang, W. Li, X. Chen, Highly enhanced electrocatalytic oxidation of glucose on $Cu(OH)_2/CuO$ nanotube arrays modified copper electrode, J. Solid State Electrochem. 16 (2012) 2877-2881.

[36] F. Meng, W. Shi, Y. Sun, X. Zhu, G. Wu, C. Ruan, X. Liu, D. Ge, Nonenzymatic biosensor based on Cu_xO nanoparticles deposited on polypyrrole nanowires for improving detection range, Biosens. Bioelectron. 42 (2013) 141-147.

[37] Y. Zhao, J. Zhao, D. Ma, Y. Li, X. Hao, L. Li, C. Yu, L. Zhang, Y. Lu, Z. Wang, Synthesis, growth mechanism of different Cu nanostructures and their application for non-enzymatic glucose sensing, Colloids Surf., A 409 (2012) 105-111.

[38] J. Zhao, F. Wang, J. Yu, S. Hu, Electro-oxidation of glucose at self-assembled monolayers incorporated by copper particles, Talanta 70 (2006) 449-454.

[39] X. Kang, Z. Mai, X. Zou, P. Cai, J. Mo, A sensitive nonenzymatic glucose sensor in alkaline media with a copper nanocluster/multiwall carbon nanotube-modified glassy carbon electrode, Anal. Biochem. 363 (2007) 143-150.

[40] S. Cherevko, C.H. Chung, The porous CuO electrode fabricated by hydrogen bubble evolution and its application to highly sensitive non-enzymatic glucose detection, Talanta 80 (2010) 1371-1377.

[41] P. Zhang, L. Zhang, G. Zhao, F. Feng, A highly sensitive nonenzymatic glucose sensor based on CuO nanowires, Microchim. Acta 176 (2012) 411-417.

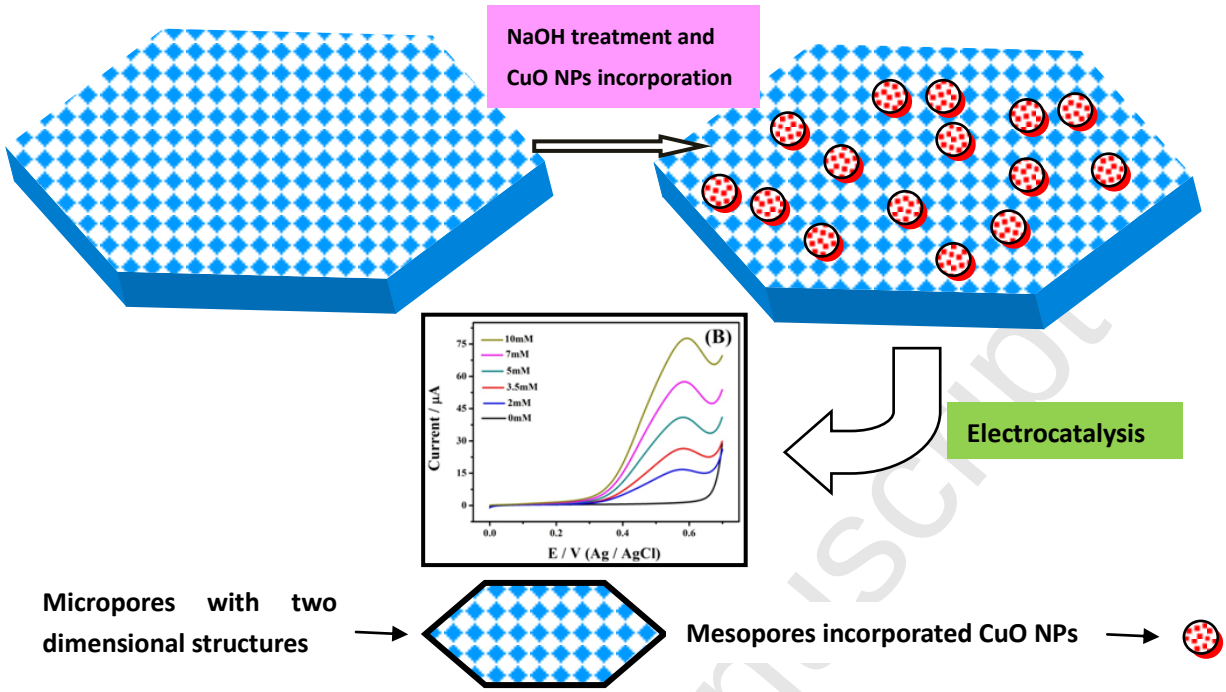

Highlights

- The hierarchical zeolite has micro/meso bimodal pore structures.
- High content of CuO NPs were incorporated into the hierarchical zeolite.
- The modified electrode exhibits the excellent electrocatalysis to glucose oxidation in alkaline.

Table 1 Textural properties of meso-MFI samples before and after loading CuO NPs

Samples	Surface area (m^2/g)	Pore volume (cm^3/g)		
	BET	Total	Micro	Meso
meso-MFI	267	0.286	0.089	0.198
meso-MFI-15%CuO	135	0.087	0.061	0.026

Table 2 Comparison of the performance of the meso-MFIOH-15%CuO glucose sensor with that of non-enzymatic glucose sensors base on Cu or Cu oxide nanomaterials.

Electrodes	Potential (V)	Linear range (M)	Detection limit (M)	Reference
CuO/graphene	0.60	1.0×10^{-6} — 8.0×10^{-3}	1.0×10^{-6}	[20]
CuO/SBA-15	0.58	1.0×10^{-5} — 2.0×10^{-2}	1.0×10^{-5}	[21]
CuO nanocubes/graphene	0.59	2.0×10^{-6} — 4.0×10^{-3}	7.0×10^{-7}	[29]
CuO NPs	0.55	5.0×10^{-6} — 2.3×10^{-3}	5.0×10^{-7}	[32]
CuO/TiO_2	0.70	1.0×10^{-5} — 2.0×10^{-3}	3.9×10^{-7}	[33]
flower-shaped CuO	0.58	1.0×10^{-5} — 1.0×10^{-2}	1.3×10^{-6}	[34]
$Cu(OH)_2$/CuO nanotube arrays	0.80	1.0×10^{-6} — 1.0×10^{-3}	5.0×10^{-7}	[35]
Cu_xO/PPy/Au	0.60	0—8×10^{-3}	6.2×10^{-6}	[36]
Cu flowers	0.70	2.0×10^{-6} — 7.5×10^{-5}	1.0×10^{-6}	[37]
Cu NPs	0.70	3.0×10^{-6} — 1.0×10^{-2}	7.0×10^{-7}	[38]
Cu nanocluster/MWCNTs	0.65	7.0×10^{-4} — 3.5×10^{-3}	2.1×10^{-5}	[39]
Porous CuO	0.65	1.0×10^{-6} — 2.5×10^{-3}	1.4×10^{-7}	[40]
meso-MFI-15%CuO	0.65	5.0×10^{-7} — 1.84×10^{-2}	3.7×10^{-7}	This work

Figure Captions

Fig. 1A XRD patterns of meso-MFI samples after loading 0% CuO (a), 5% CuO (b), 10% CuO (c) and 15% CuO (d). (▽denoted as the diffraction peaks of CuO).

Fig. 1B N_2 sorption isotherms of meso-MFI before (a) and after (b) loading 15% CuO. The inset is pore size distribution of meso-MFI.

Fig. 2 TEM images of meso-MFI samples loading 5% CuO (A and B), 10% CuO (C and D), and 15% CuO (E and F).

Fig. 3 Amperometric responses of glucose on 15% CuO/meso-zeolite (a), 15% CuO/SBA15 (b) and 15% CuO/micro-zeolite (c).

Fig. 4 (A) Cyclic voltammograms of the meso-MFI-15% CuO modified electrode in the presence and absence of 5 mM glucose in 100 mM NaOH and scan rate at 50 mV/s; (B) LSV obtained for the increment of glucose (from 0 mM to 10 mM) on meso-MFI-15% CuO modified electrode in 0.1 M NaOH and scan rate at 50 mV/s; (C) Cyclic voltammograms of 5 mM glucose at the different scan rate. Inset: the plot of anodic peak currents *vs.* scan rates.

Fig. 5 (A) Amperometric responses of meso-MFI-15% CuO electrode to the successive additions of glucose from 0.5 μM to 18.4 mM (triple injections per concentration) in 100 mM NaOH and the applied potential of 0.65 V; (B) The corresponding calibration curve.

Fig. 6 Amperometric responses of meso-MFI-15% CuO modified electrode to 0.5 mM glucose in various concentrations of NaOH (A), at different applied potentials (B), and different CuO loadings (C).

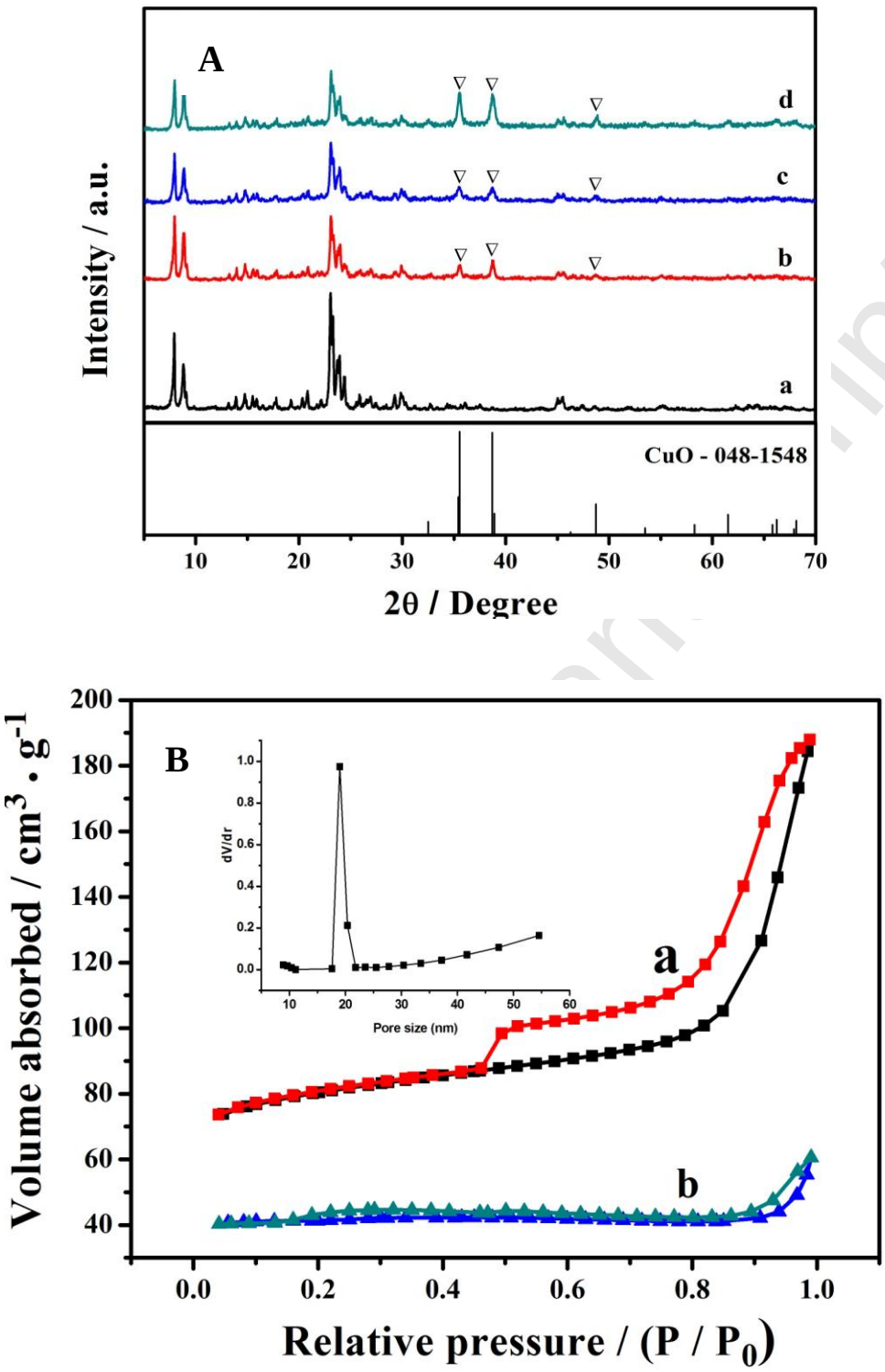

Fig. 1A XRD patterns of meso-MFI samples after loading 0% CuO (a), 5% CuO (b), 10% CuO (c) and 15% CuO (d). (▽denoted as the diffraction peaks of CuO).

Fig. 1B N_2 sorption isotherms of meso-MFI before (a) and after (b) loading 15% CuO. The inset is pore size distribution of meso-MFI.

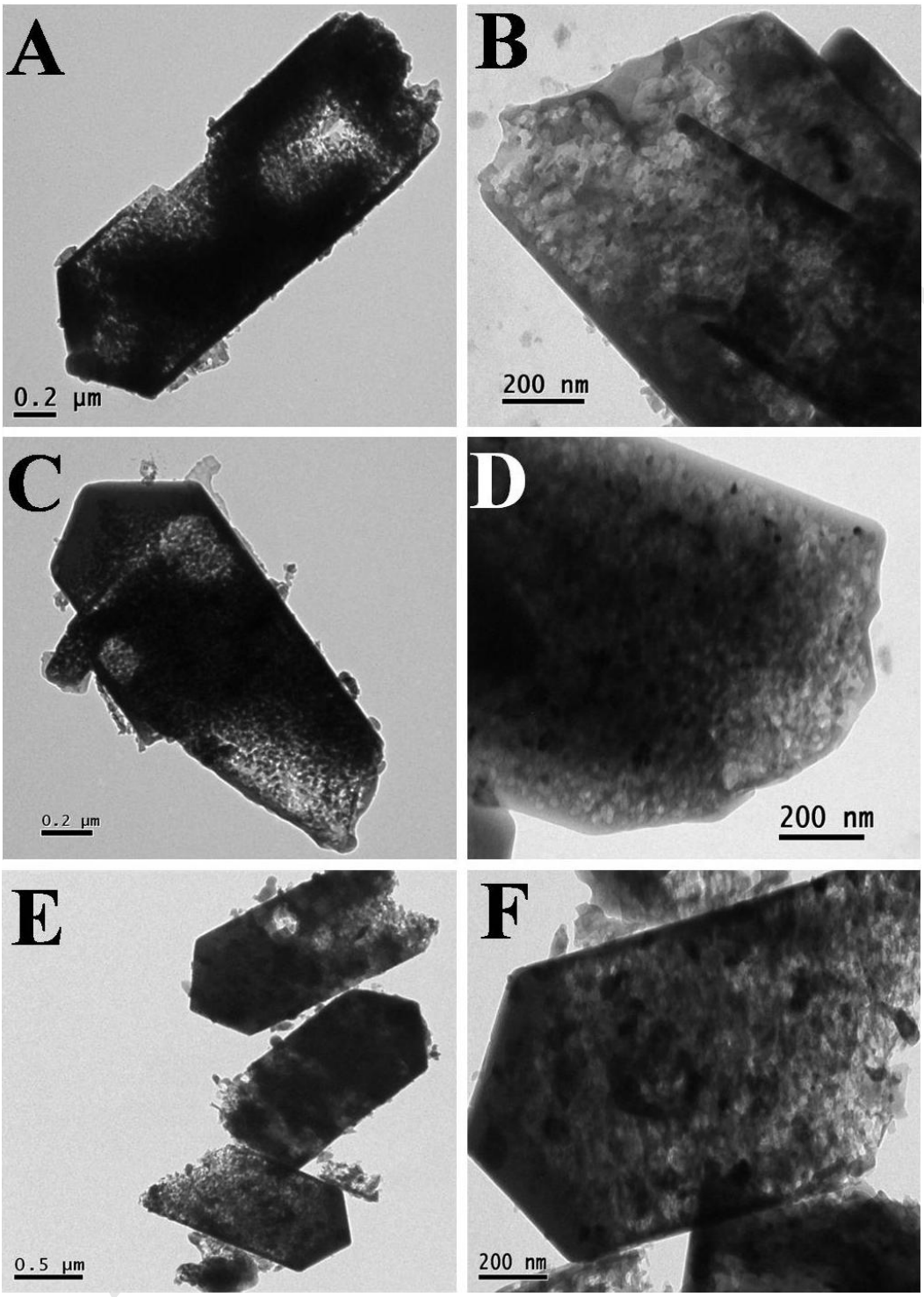

Fig. 2 TEM images of meso-MFI samples loading 5% CuO (A and B), 10% CuO (C and D), and 15% CuO (E and F).

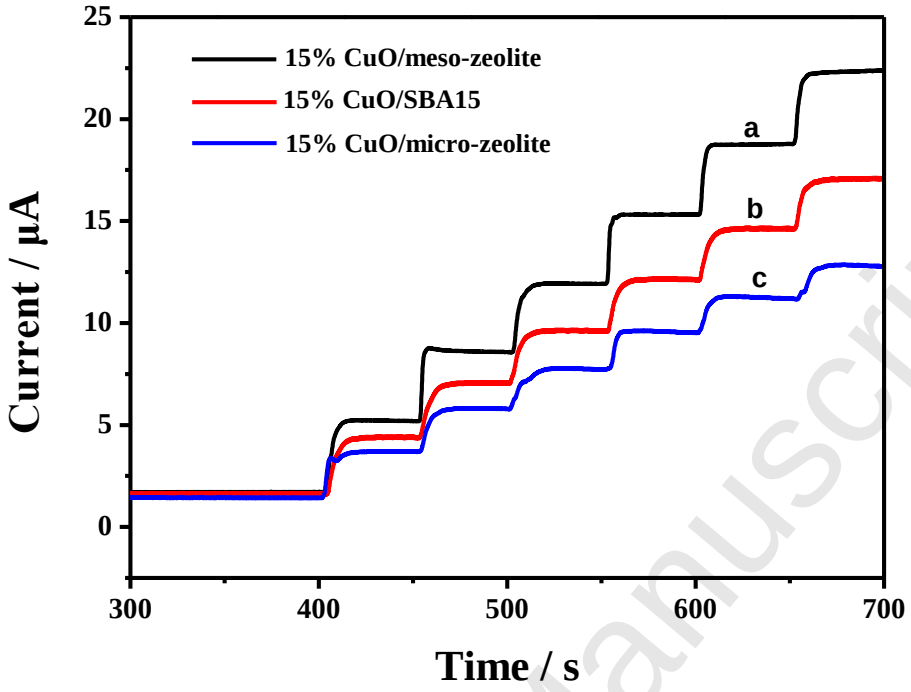

Fig. 3 Amperometric responses of glucose on 15% CuO/meso-zeolite (a), 15% CuO/SBA15 (b) and 15% CuO/micro-zeolite (c).

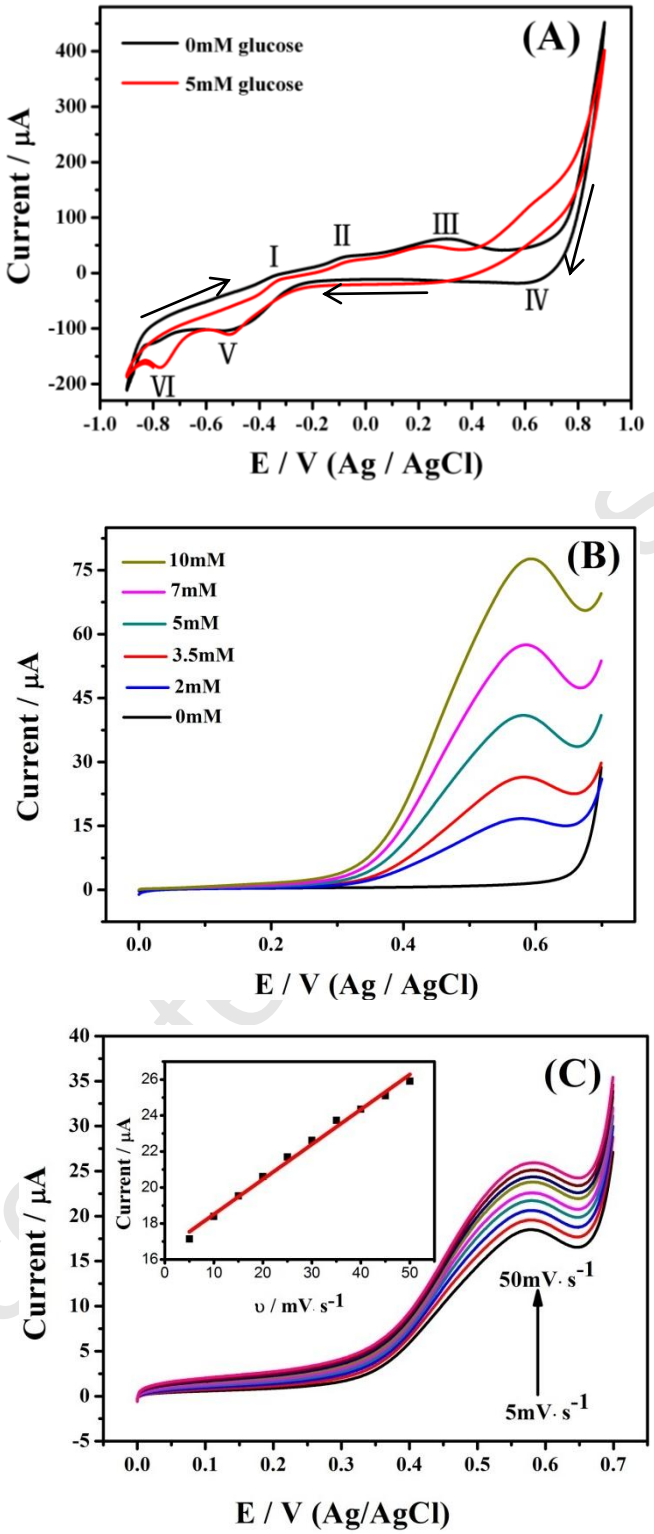

Fig. 4 (A) Cyclic voltammograms of the meso-MFI-15% CuO modified electrode in the presence and absence of 5 mM glucose in 100 mM NaOH and scan rate at 50 mV/s; (B) LSV obtained for the increment of glucose (from 0 mM to 10 mM) on meso-MFI-15% CuO modified electrode in 0.1 M NaOH and scan rate at 50 mV/s; (C) Cyclic voltammograms of 5 mM glucose at the different scan rate. Inset: the plot of anodic peak currents *vs.* scan rates.

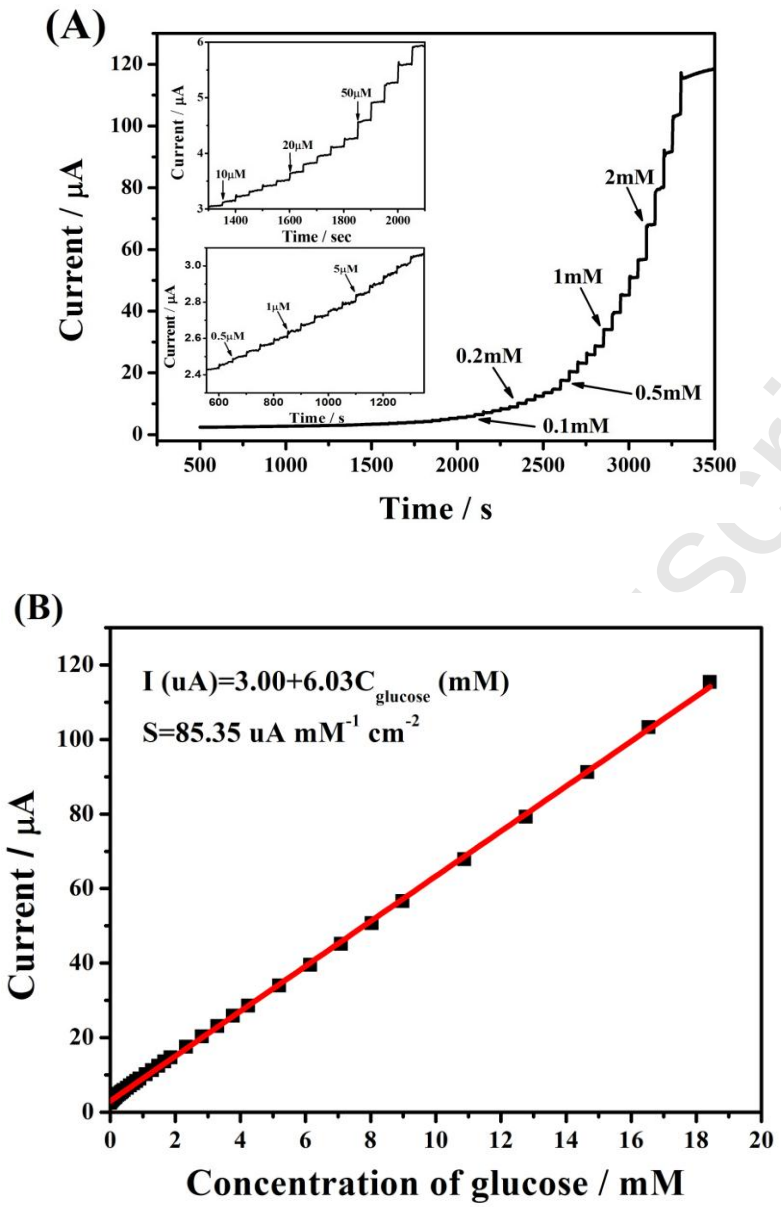

Fig. 5 (A) Amperometric responses of meso-MFI-15% CuO electrode to the successive additions of glucose from 0.5 μM to 18.4 mM (triple injections per concentration) in 100 mM NaOH and applied potential of 0.65 V; (B) The corresponding fitting curve.

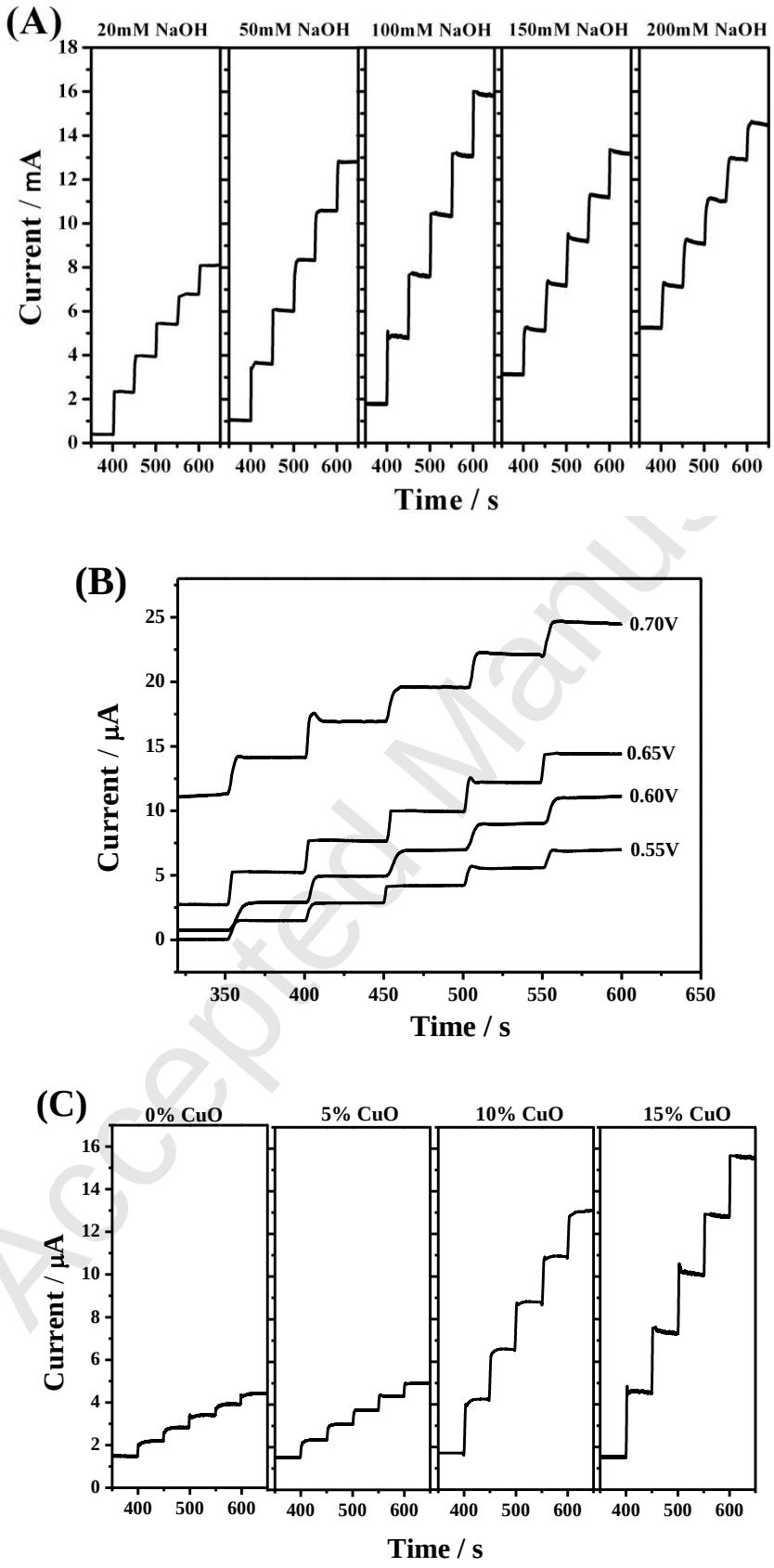

Fig. 6 Amperometric responses of meso-MFI-15% CuO modified electrode to 0.5 mM glucose in various concentrations of NaOH (A), at different applied potentials (B), and different CuO loadings (C).